A Decision Support System to Enhance Electricity Grid Resilience against Flooding Disasters

Hassan Tavakol-Davani (hdavani@sdsu.edu)
San Diego State University https://orcid.org/0000-0001-5428-4844
Michael Violante
San Diego State University
Saeed Manshadi
San Diego State University

Research Article

Keywords: Decision Support System, Flood Control, Utility Poles, Mathematical Programming, Power System, Resilience

Posted Date: January 14th, 2022

DOI: https://doi.org/10.21203/rs.3.rs-1000967/v1

A DECISION SUPPORT SYSTEM TO ENHANCE ELECTRICITY GRID RESILIENCE AGAINST FLOODING DISASTERS

Hassan Tavakol-Davani, PhD, P.E., Assistant Professor, Department of Civil, Construction & Environmental Engineering, San Diego State University (hdavani@sdsu.edu),
Michael Violante, Graduate Student, Department of Civil, Construction & Environmental Engineering, San Diego State University (mviolante@sdsu.edu),
Saeed D. Manshadi, Ph.D, Assistant Professor, Department of Electrical & Computer Engineering, San Diego State University (smanshadi@sdsu.edu)
Corresponding author: Hassan Tavakol-Davani, Ph.D, P.E. (hdavani@sdsu.edu)
Postal address for all authors: 5500 Campanile Dr, San Diego, CA 92182

Abstract: In different areas across the U.S., there are utility poles and other critical infrastructure that are vulnerable to flooding damage. The goal of this multidisciplinary research is to assess and minimize the probability of utility pole failure through conventional hydrological, hydrostatic, and geotechnical calculations embedded to a unique mixed-integer linear programming (MILP) optimization framework. Once the flow rates that cause utility pole overturn are determined, the most cost-efficient subterranean pipe network configuration can be created that will allow for flood waters to be redirected from vulnerable infrastructure elements. The optimization framework was simulated using the Julia scientific programming language, for which the JuMP interface and Gurobi solver package were employed to solve a minimum cost network flow objective function given the numerous decision variables and constraints across the network. We implemented our optimization framework in three different watersheds across the U.S. These watersheds are located near Whittier, NC; Leadville, CO; and London, AR. The implementation of a minimum cost network flow optimization model within these watersheds produced results demonstrating that the necessary amount of flood waters could be conveyed away from utility poles to prevent failure by flooding.

Keywords: Decision Support System**,** Flood Control, Utility Poles, Mathematical Programming, Power System, Resilience

Highlights:

1.) A decision support system framework based on network cost minimization is proposed to divert flood waters from flood-susceptible utility poles, thereby enhancing electricity grid resilience.

2.) This optimization framework is evaluated in three different watersheds in the United States using state-of-the-art mathematical optimization platforms, i.e. JuMP/Julia interface and the Gurobi solver.

3.) The results of this proposed optimization framework could provide adequate flood diversion capacity to prevent failure of utility poles.

1. INTRODUCTION

In modern society, the electricity grid is one of the vital cornerstones of socio-economic prosperity. Humans rely on an uninterrupted supply of electricity for an ever-increasing plethora of needs (Pant et al. 2018). When these needs are unmet, the consequences are often severe and range from social disruption to loss of property and life.

In many cases, it is not only the socio-economic activity of communities that is affected by electricity grid failures. Studies by (Anderson & Bell 2012), (Klinger et al. 2014) and (Marx et al. 2006) all present similar evidence pointing to sharp increases in mortality risk and disease during periods of blackout. Each of these studies refer to one particularly devastating blackout during August 14-15th, 2003 in New York City. During this time, death, illness, and injury greatly increased due to food poisoning, hypothermia, falling, and the inability to contact health care providers. The multitude of adverse effects caused by power outages on communities in the U.S. and around the world is a rapidly evolving field of research with a wide availability of literature.

There has been an unfortunate recurrence of disasters (separate from the incident in New York) caused by electricity grid failures in recent years (Campbell & Lowry 2012). According to a University of Vermont study (Hines et al. 2008), from 1984-2006, there have been 933 reported power outage events in the U.S., most of which were sustained (lasting longer than 5 minutes) and wind/rain events causing damage to utility poles and other electricity infrastructure were one of

the leading causes. U.S. utility companies are legally obligated to disclose to the North American Electric Reliability Corporation (NERC) any electricity grid irregularities and/or disruptions exceeding 300 Megawatts (MW) and impacting 50,000 customers or more. During this 22-year period, it was estimated that over 185,000 individuals were without power and adversely affected by power outages caused by wind/rain. It is likely the weather-related figures are underreported because not all weather-related power outages were accurately reported by utility companies to NERC (Campbell & Lowry 2012). Therefore, the actual number of people impacted by weather-related power outages is likely significantly higher.

Another study conducted by the U.S. Department of Energy (DOE), which has its own database of grid disruption occurrences, demonstrates that during an 18-year period (1992-2010) 78% of 1,333 recorded sustained grid disruptions were weather-related (severe rain and wind). It is estimated that these disturbances affected over 178 million customers over the course of the 18-year period (Campbell & Lowry 2012).

In many cases, the vulnerabilities of U.S. electrical infrastructure are only examined and given necessary attention after these disasters occur (Hemme 2015). Antiquated electrical infrastructure in the U.S. has also produced concerns over national security over the past 20 years. Under current circumstances, U.S. infrastructure is divided into sixteen critical, interrelated, and interdependent sectors, including the electricity grid. Therefore, a natural disaster could be sufficient to cripple not only the electricity grid, but other infrastructure sectors as well, according to Hemme (2015). To address these concerns, recent publications proposed cost-efficient MILP frameworks to enhance resilience of electricity and natural gas elements of microgrids against various types of disturbances, including natural disasters (Manshadi & Khodayar 2015, 2018). The

84 results of these two studies provided novel approaches for microgrid operators to contend with
85 disturbances based on different simulated outcomes.

86 The increasing dependence on an aging electricity grid that has become significantly less
87 reliable over the past several years (Li & Guo 2006) and averting potential disaster when elements
88 of this grid (e.g., power poles) fail were the primary motivations for conducting this study.

89 This paper particularly focuses on increasing electricity grid resilience by mitigating
90 utility pole failure due to flooding. Figure 1 illustrates an example of such a failure.

91
92 **Fig 1.** Utility poles failing from flood waters due to heavy rainfall causing dam overtopping in Sanford, Michigan
93 (McLaughlin 2020)
94
95 To mitigate utility pole failure, each watershed is mathematically modeled as a network,
96 a system of links and nodes, which can be used to find optimal solutions by optimizing cost, ease
97 of use, failure, energy efficiency, etc. All flow networks have three different types of nodes:
98 production, storage, and consumption (Turnquist & Vugrin 2013). Also, as seen in (Crucitti et al.
99 2004), not all nodes are created equally, they will have varying capacities based on node type and
100 the composition of the network. Specifically, a minimum-cost network flow methodology is used

in this study. This approach was selected because network optimization has proven to be effective across a variety of disciplines.

Recently, there have been optimization procedures applied to watershed management for pollution control best management practices, e.g. (Maringanti et al. 2011), (Muleta & Nicklow 2002) and optimal allocation of water inside distribution networks using various techniques. It does not appear as though a minimum cost network flow optimization problem has been applied to a stream network inside a watershed to optimally redirect flood waters away from utility poles.

However, in the past several decades, there has been much research conducted on water allocation in river basins via network flow programming. One of the earliest network flow algorithms for watershed planning purposes was developed by (Evenson & Moseley 1970). An "out-of-kilter" algorithm was introduced in 1976 for optimizing a multi-reservoir network for hydropower and water usage along the Trent River in Ontario, Canada (Sigvaldson 1976).

As years went on, optimization models for watershed management became increasingly more sophisticated (Ilich 2009). Watershed planning and management models underwent significant advancements in the 1980's and 1990's, with the introduction of programs like, MODSIM3. This was a decision support system based on a network optimization model that allowed the City of Fort Collins, Colorado to more efficiently meet water demands (Labadie et al. 1986). Six years later, a network flow model called KCOM integrated both surface and subterranean water allocation for Kern County, CA, which allowed for thorough and extensive optimization of the water distribution network in the Kern County Water Bank (Andrews et al. 1992).

Although mixed-integer linear programming (MILP) is not a recent technique (Bixby 2012), its application in water resources planning and management has contributed to important

advancements in recent years. (Liu et al. 2011) used a MILP approach to meet water usage demands and determine the most cost-efficient placement of water resources infrastructure on the Greek Islands of Paros-Antiparos and Syros. (Veintimilla-Reyes et al. 2016) adopted MILP to a network optimization problem to create a model addressing water accessibility concerns by predicting appropriate amounts of water in reservoirs at different times of the day. (Watson et al. 2004) demonstrates that several unique optimization objectives must be considered to realize the optimal configuration of sensor placement for safeguarding water distribution networks. (Mani et al. 2016) proposed a mixed integer linear fractional programming approach in Northern Louisiana to both maximize groundwater usage and minimize reservoir storage capacity using four existing surface water reservoirs. Groundwater usage was further optimized via conjunctive use with the surface water reservoirs.

The optimization of water distribution operations is by no means a new research topic. However, optimal allocation of drinking water has become an extremely important consideration in recent years because of the increasing scarcity of potable water. Studies utilizing both linear and non-linear programming (Carini et al. 2018) have been successful in minimizing cost while ensuring drinking water is efficiently and safely transported through networks to where it is most needed (Bieupoude et al. 2012). Municipal water distribution systems have also been modeled using "multi-period mixed integer linear programming" to find cost-efficient solutions and meet both potable and non-potable consumer needs (Ghelichi et al. 2018). A successful, large-scale instance of multi-period mixed integer linear programming in a water distribution system is found in Kuwait where the model was applied to energy and water co-generation (Alqattan 2014).

This study utilizes a MILP optimization framework as a decision support system to alleviate flooding impacts on utility poles that are at risk of failure. Our model for a node receives

147 flood water from the surface and conveying the flow through a network system of pipe to a
148 discharge point. This type of conveyance occurs only at nodes where drainage is occurring.
149
150 The methodology proposed in this study aims to create a versatile decision support
151 framework that will redirect flood waters produced from multiple return periods of storms away
152 from flood-susceptible utility poles through a cost-efficient network of subterranean pipes. For
153 each watershed, storm return periods ranging from 2-500 years are individually analyzed at each
154 at-risk utility pole to determine which storm return period(s) cause utility pole failure. The
155 techniques used for obtaining peak flow rates in subwatersheds and subsequently determining
156 results for the utility pole pass/fail analysis are further elaborated in the methodology section.
157 Even though the results of this study represents utility pole failure under some of the worst-
158 case scenario storms, the unprecedented role of climate change in causing these types of "rare"
159 storms to occur more frequently has become well-documented. Recent studies by (Lubchenco &
160 Hayes 2012), (Trenberth 2011), and (Teegavarapu 2017) confirm with overwhelming evidence
161 that there is a connection between climate change and the increasing frequency of more powerful
162 storms recorded in the U.S. in the past few decades. Many of these more intense precipitation
163 events occurred east of the Rocky Mountains (Groisman et al. 2012). Since more powerful storms
164 are indisputably occurring more often, developing novel approaches to enhance the resilience of
165 utility poles and the electricity grid against extreme events is of paramount importance at the
166 present time. A 100-year storm is the extreme event of interest for this paper.
167 This paper contains the following structure: First, the anatomy of the minimum-cost network
168 flow model is discussed with respect to each watershed. Then, the methodology is presented for
169 how each of the peak flow rate inputs to the model is obtained. Subsequently, the minimum cost
170 network optimization problem is introduced, and the decision variables, objective function and

171 constraints are defined. Lastly, an analysis of the results for each study area is discussed and
172 conclusions are drawn based upon the outputs for the model corresponding to each study area.
173

174 # 2. METHODOLOGY

175 ## 2.1. Study Areas and Hydrologic Analyses

176

177 The three watersheds in this paper, Whittier, NC; Leadville, CO; and London, AR, were
178 selected because each are located in underserved areas and contain utility poles susceptible to
179 failure during flood events. These watersheds were delineated using USGS's (U.S. Geological
180 Survey) Streamstats tool and ArcGIS 10.6.1 with publicly available 10-m Digital Elevation
181 Models (DEMs) from USGS. The Archydro add-on for ArcGIS 10.6.1 was used to delineate
182 subwatersheds inside each watershed.

183 These subwatersheds each have one longest, aggregate flow path (link). Between each link
184 is a node. Therefore, the number of subwatersheds delineated inside of a watershed determines the
185 composition of the surface node-link network that will be inputted into the optimization model.

186 Stormwater draining into nodes is modeled to be conveyed through pipes extending
187 downward at a vertical slope to connect with larger diameter pipes that will convey the flow to the
188 most downstream node of the network, i.e. the outfall.

189 The underground network mirrors the surface network, with the pipe extending from
190 drainage nodes connecting the two. Once the model has run, the optimal underground links are
191 selected, based on projected cost, runoff calculated for each subwatershed and the calculated flow
192 rates at which the utility poles fail. These criteria function as the basis for the decision support
193 system.

The Whittier, NC watershed spans an area of 390.4 acres (1.58 sq. km) (Fig 2) and drains into the Tuckasegee River. This watershed is comprised of 31 subwatersheds and 4 utility poles susceptible to failure by flooding. The soil in this watershed is predominantly hydrologic type C. Delineation was performed from the utility pole (green dot) located closest to the Tuckasegee River (Fig 2). The nodes labeled in this figure will be used in the model.

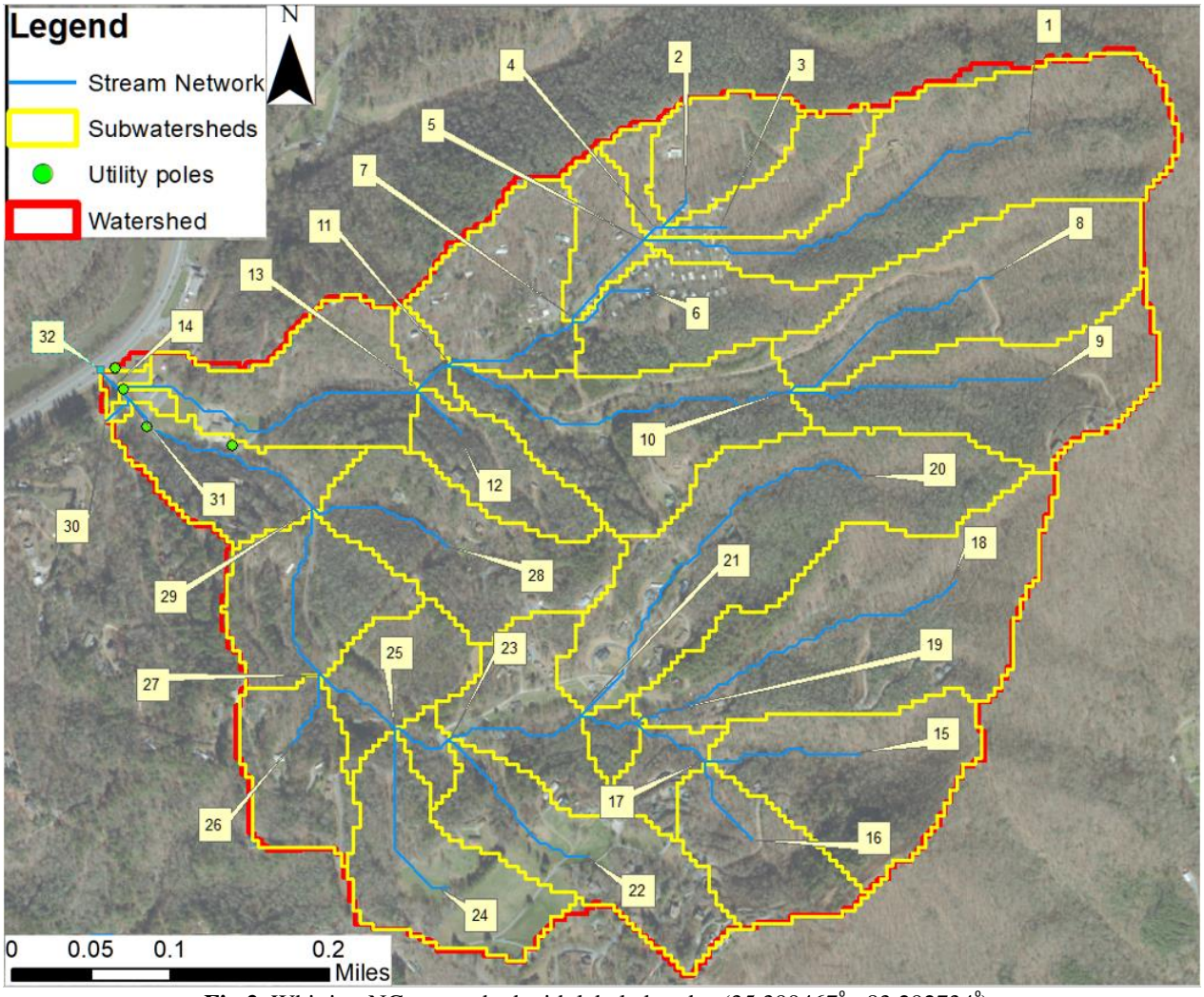

Fig 2. Whittier, NC watershed with labeled nodes (35.399467°, -83.292734°)

Runoff in the Whittier, NC watershed was calculated using the Rational Method because each subwatershed has an area (A) sufficiently small (<200 acres) to warrant using this hydrologic method.

$$Q = C_f CIA \quad (1)$$

Where Q is the peak flow rate of a storm in a subwatershed. The runoff coefficient (C) is assumed to be 0.25 due to the watershed being in a predominantly wooded area (Charlotte-Mecklenburg Stormwater Services 2014). When a storm has a return period between 25 years and 100 years, the Charlotte-Mecklenburg Stormwater Design Manual dictates that a frequency factor (C_f) must be applied to the rational formula. The average time of concentration for all subwatersheds was approximately 6.3 minutes. Assuming storm duration is equal to the time of concentration, the data in (U.S. Geological Survey et al. 2006) can be used in conjunction with NOAA Atlas 14 precipitation intensity data to interpolate an appropriate intensity for a 6.3-minute storm.

The rainfall intensity (I), which is portrayed in units of inches/hour, is determined from Intensity-Duration-Frequency (IDF) curves. These curves represent parameters that were combined into the following empirical equation.

$$Intensity\ (I) = \frac{a}{(t+b)^n} \quad (2)$$

In equation 2, t represents the extent of rainfall (minutes), which is equal to the time of concentration for each subwatershed. The variables a, b, and n are empirically determined storm-fitting parameters enumerated in Charlotte-Mecklenburg Stormwater Design Manual. Time of concentration was calculated using the Kirpich equation.

$$t_c = (0.0078 * (\frac{L^{0.77}}{S^{0.385}})) * 2 \quad (3)$$

Equation 3 is multiplied by 2 because the overland flow is occurring over predominantly grassed surfaces.

The Charlotte-Mecklenburg Stormwater Design Manual was used for hydrological calculations in the Whittier, NC watershed because it is the most comprehensive hydrology manual

of any large city near Whittier. It is also assumed that the terrain in Charlotte is hydrologically similar enough to Whittier for the formulae and their respective variables to be valid.

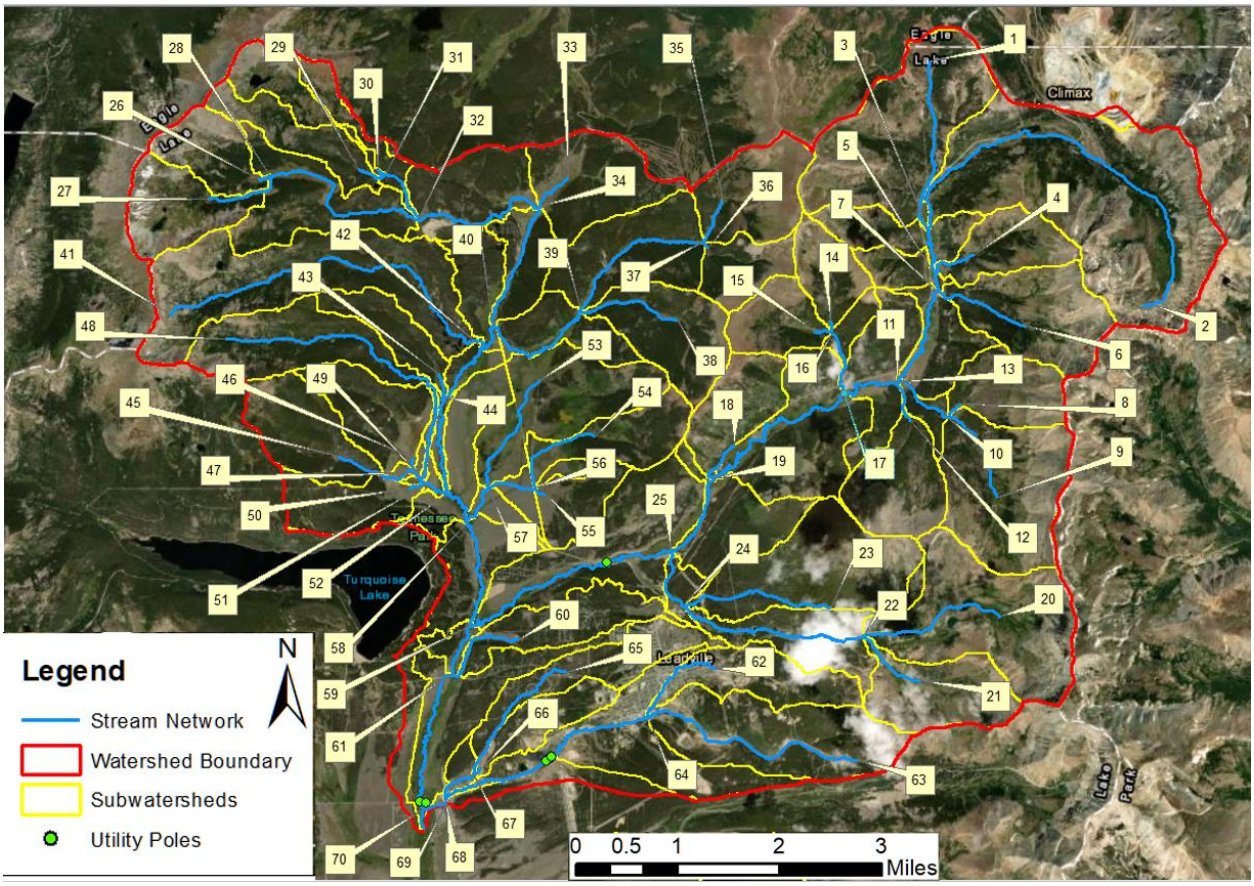

Fig 3. Leadville, CO watershed with labeled nodes (39.222713°, -106.356648°)

The second watershed is much larger and is located near Turquoise Lake in Colorado with an area of 113 sq. miles (292.67 sq. km) and 69 sub watersheds (Fig 3). Two of the watershed's major streams flow through the town of Leadville. Additionally, there are 6 flood-susceptible utility poles across three locations. This entire watershed stream network ultimately drains into the Arkansas River.

Each subwatershed has an area greater than 200 acres and requires the "Natural Resource Conservation Service (NRCS) Curve Number Loss and Dimensionless Unit Hydrograph Method" to accurately calculate the peak flow of each sub watershed (City of Colorado Springs 2014). The City of Colorado Springs Drainage Criteria Manual Vol I was used because Leadville and

241 surrounding areas are not densely populated and do not have established hydrology/drainage
242 manuals.

243 $$Q = \frac{(P-0.2S)^2}{(P+0.8S)} \quad (4)$$

244 In equation 4, Q is the accumulated runoff (in) and is calculated with the accumulated
245 rainfall depth (P) and approximate soil retention (S). The variables P and S are both expressed in
246 units of inches. The equation for approximate soil retention is conveyed as:

247 $$S = \left(\frac{1000}{CN}\right) - 10 \quad (5)$$

248 A spatially averaged curve number was developed for each subwatershed by synthesizing
249 NRCS land use and Soil Survey Geographic database (SSURGO) soils data, following the
250 methodology introduced in (Merwade 2010). The majority of subwatershed curve numbers were
251 within the 60-70 range. This methodology for determining spatially averaged curve numbers was
252 used in the Leadville, Colorado and London, Arkansas watersheds.

253 Peak flow in a sub watershed is expressed as:

254 $$Q_P = QAQ_p \quad (6)$$

255 Where Q_p is the unit peak discharge (cfs/mi^2), which is calculated using the following
256 formula.

257 $$Q_p = \frac{(484)*AQ}{(0.67*t_c)} \quad (7)$$

258 The constant, 484, is the unit hydrograph peak rate factor. This factor remains constant in
259 equation 7. In the NRCS method, the time of concentration (t_c) is equal to the sum of the
260 concentrated flow travel time (T_t) and the overland flow time (T_i).

261 Concentrated flow travel time is determined from the following equation.

262 $$T_t = \frac{L}{(3600*V)} \quad (8)$$

L is the length of the flow path, V is velocity (ft/s) and 3600 is a conversion from seconds to hours. The equation for overland flow time is written as follows.

$$T_i = \frac{0.007(nL)^{0.8}}{P^{0.5}\, S^{0.4}} \quad (9)$$

In equation 9, n is the manning's roughness coefficient, which is assigned based on the material the channel is made from. Since it is assumed all channels in the Leadville Colorado watershed are natural, a manning's roughness coefficient of either 0.15 for "short prairie grass", 0.24 for "dense grass", or 0.8 for "dense underbrush" was used based on observations made using google earth and guidelines provided in the City of Colorado Springs Drainage Criteria Manual.

The precipitation depth for a 2-year, 24-hour duration storm (P) is also used in equation 9. S is the slope of the hydraulic grade line of the channel.

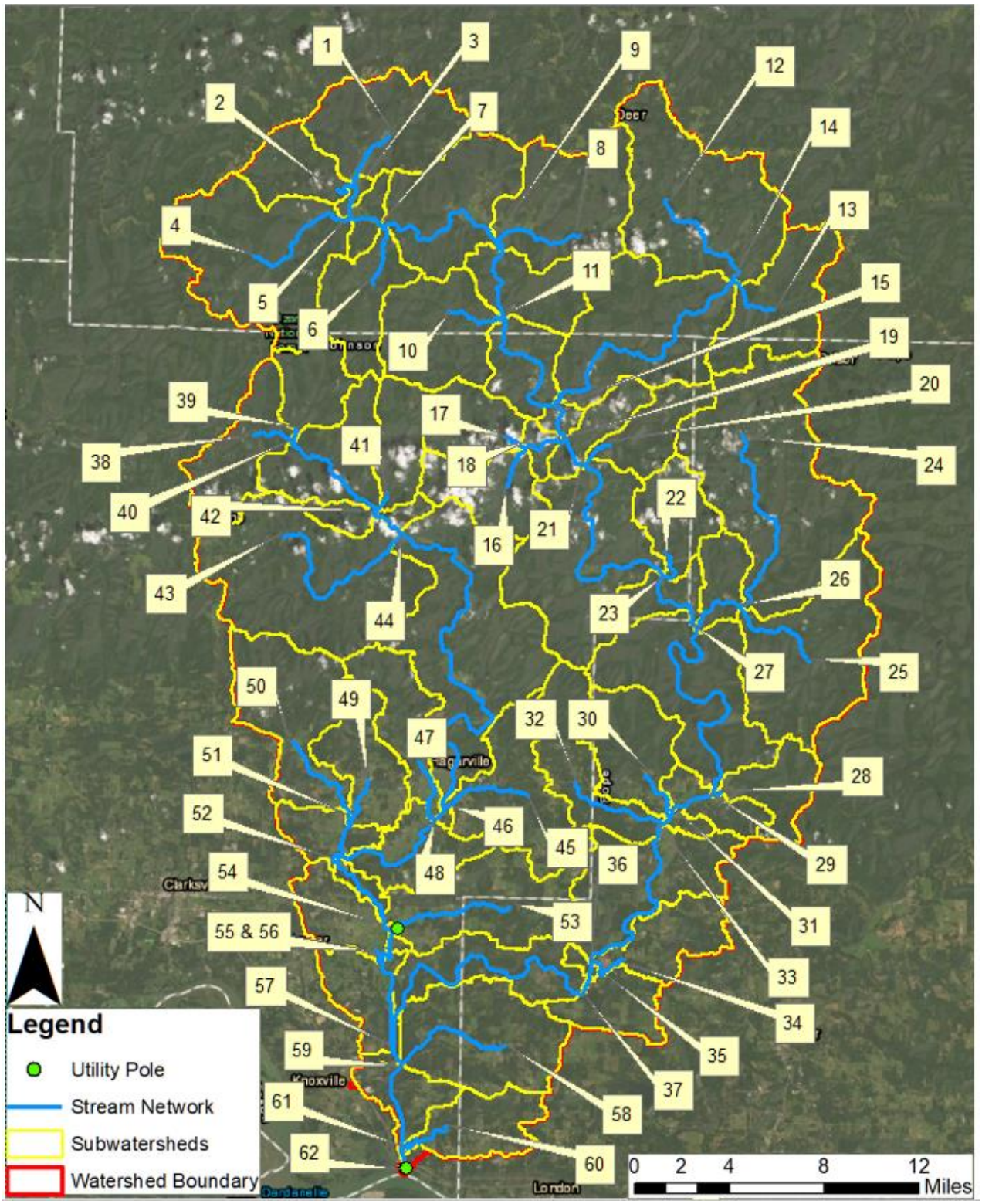

Fig 4. London, Arkansas watershed with labeled nodes (35.345107°, -93.329761°)

The final watershed, located in Arkansas, discharges into the Arkansas River, near the town of London. Encompassing an area of 537 sq. mile (1390.82 sq. km), this watershed stretches across a portion of the Ozark National Forest and has a major stream flowing through the town of Hagarville (Fig 4). In this watershed, there are only 61 subwatersheds, despite being larger than the Leadville Colorado watershed. There are also 3 utility poles deemed to be flood susceptible. Like the second study area, the NRCS method was used to calculate the runoff for each of the subwatersheds, using nearly the exact same formulae and methodology. In this instance, the unit peak discharge is not used to calculate peak flow. Instead, the result of Equation 4 is converted to feet, multiplied by the subwatershed area, and then divided by 24 hours. The NRCS methodology for the London, Arkansas watershed was performed in accordance with the City of Fayetteville Drainage Criteria Manual (City of Fayetteville Engineering Division 2014).

2.2. Pole Failure Model

The following assumptions were made for all utility poles:

1.) Utility pole-soil interactions can be modeled as a small retaining wall subjected to a passive pressure earth force (equation 11), which contributes to the total resisting moment. This total resisting moment opposes the moment created by the force applied by stormwater equation 10 and the WSE.

2.) The governing hydrostatic formula,

$$F = \rho Q V \tag{10}$$

is used to calculate the applied (horizontal) force from stormwater. The velocity (V) is dissipated after colliding with a utility pole.

3.) A utility pole behaves as a rigid body, as described in (Davisson & Prakesh 1963) and (Keshavarzian 2002).

4.) Full setting depth is determined by the commonly accepted rule, 10% of the utility pole length plus two feet (Keshavarzian 2002).

5.) All utility poles are directly buried in the soil with no embedment foundation, based on observations made in Google Street View.

6.) The version of the Rankine passive earth pressure force of the soil (equation 11) was used based on the assumption that the soils in each watershed are predominantly granular (Das 2016, pp. 593–645).

$$P_p = 0.5(K_p)\gamma H^2 \quad (11)$$

Assumption 6 was confirmed with an online U.S. Department of Agriculture (USDA) Natural Resources Conservation Service (NRCS) Web Soil Survey analysis in areas near the utility poles.

Passive earth pressure exists when a lateral force is causing a retaining wall to move toward the soil (Das, 2016 pp. 593–645). Gamma (γ) is the bulk density of soil and in this study, is estimated based on the soil texture and observed vegetation around utility poles (Table 1). There are several in-situ methods for accurate estimation of soil bulk density (Al-Shammary et al. 2018). However, these methods are outside the scope of this network optimization research.

Table 1. Bulk densities assigned to each watershed based on dominant soil texture and vegetation (USDA NRCS n.d.)

Watershed	Dominant Soil Texture	Amount of vegetation	[1]Bulk Density (g/cm^3)
Whittier, NC	Sandy loam	plentiful	1.40
Leadville, CO	Gravely, sandy loam	sparse	1.63
London, AR	Sandy loam	plentiful	1.40

[1]Bulk densities reported in (USDA NRCS n.d.) are in g/cm^3. During calculations these were converted to lb/ft^3.
1 g/cm^3 = 62.43 lb/ft^3

Bulk density estimates are around the upper or lower limit based on observed vegetation growth in areas around utility poles. The bulk density values were referenced from an NRCS publication (USDA NRCS n.d.).

7.) In Rankine theory, it is assumed that the structure being modeled as a retaining wall is completely vertical and has a smooth surface. Therefore, factors like wall-soil friction and retaining wall sloping are negligible (Pisani 2002).

8.) Equation 12 assumes that there is no angle of incline and only takes into consideration the angle of friction. Kp is the Rankine passive pressure coefficient, which can be calculated from the following equation.

$$K_p = tan^2(45 + \frac{\phi'}{2}) = \frac{1+sin\phi'}{1-sin\phi'} \quad (12)$$

9.) Based on (Das 2016, pp. 593–645), it is assumed the resisting force is applied at approximately 2/3 of the utility pole (retaining wall) burial depth (measured from the ground line downward), or a distance 1/3 from the bottom of the utility pole (measured upward).

The angle of friction is determined based on a soil's grain distribution size, void ratio, surface roughness, and angularity (USDA Forest Service Engineering Staff 1994). A proposed regression model (Bareither et al. 2008) calculated an average friction angle for four different types of sand based on stress-displacement performance. The average soil friction angle calculated for group 3 sands was 35° and this is consistent with values reported in USCS soil friction angle charts (Koloski et al. 1989) and in the USDA publication (USDA Forest Service Engineering Staff 1994) for sandy, non-cohesive soils.

It is assumed that each utility pole in this study will be subjected to an applied moment from stormwater at a depth varying with storm return period (WSE) and a cumulative resisting moment. This total resisting moment (M_t) is the sum of the maximum allowable moment at the utility pole groundline (M_{gl}) (equation 14) (Keshavarzian 2002) and the product of the passive pressure occurring at a depth of (2/3)H (M_p).

$$M_t = M_{gl} + M_P \quad (13)$$

$$M_{gl} = f_s * \pi * \frac{d^3}{384{,}000} \quad (14)$$

Where f_s is the fiber stress (psi) of the wood utility pole, according to the American National Standards Institute (ANSI). This value varies based on the class and species of the pole (Table 2). The diameter (d) of the utility pole at the groundline can also be expressed as

$$d = \frac{C}{\pi} \quad (15)$$

Where the circumference of the utility pole at groundline (C) is calculated as follows

$$C = C_0 + (C_1 - C_0) * (\frac{L - E}{L - 6}) \quad (16)$$

C_0 and C_1 are the circumferences of the pole at the top and 6 feet from the bottom, respectively. The total length (L) of the pole has a setting depth (E) associated with it and the constant 6 denotes 6 ft subtracted from the total length of the pole. Equations 14-16 follow the methodology used by (Keshavarzian 2002).

Table 2. Utility pole attributes for each watershed (Wolfe & Moody 1994)

Watershed	Pole Class	[1]Length Range (ft)	[1]Assumed Length (ft)	[2]Top Circ. (in)	[2]Circ. 6 ft from pole bottom (in)	[3]Fiber Stress (lb/in^2)	[1]Setting Depth (ft)
Whittier, NC	7	20 - 45	30	15	21.00	8000	5
Leadville, CO	7	20 - 45	35,45	15	22.25, 24.75	8000	5.5, 6.5
London, AR	7	20 - 45	45	15	24.75	8000	6.5

Note: Circumference denoted as "Circ."
[1]1 ft = 0.305 m
[2]1 in = 2.54 cm
[3]1 lb/in^2 = 6.89 kPa

In Table 2, the Southern Pine pole species was assumed for all utility poles because that is the species of wood used for most utility poles in North America (Wolfe & Moody 1994). Assumed utility pole lengths were estimated from a google street view analysis. Circumference 6 feet from the pole bottom was determined using a circular taper factor of 0.25 in/ft. Setting depth was determined using the 10% of total length plus two feet rule.

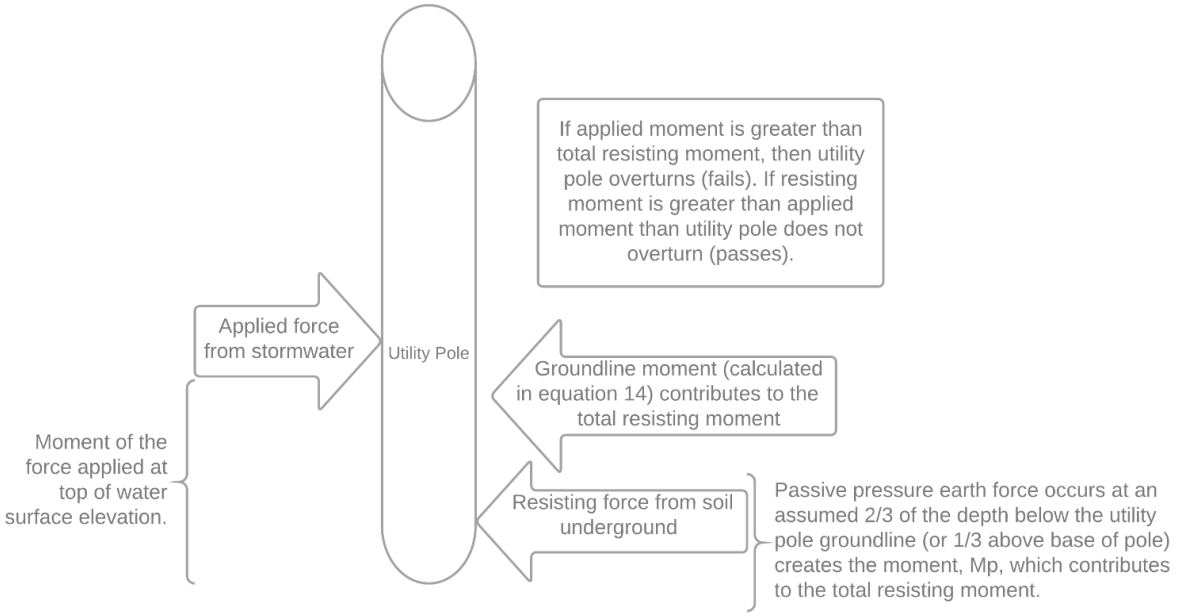

Fig 5. Diagram depicting forces occurring on utility pole from soil and stormwater

Figure 5 depicts the culmination of the hydrostatic and geotechnical calculations. The accumulated flow from each subwatershed along a stream is used to calculate the applied moment on a utility pole. The same calculations were performed for every at-risk utility pole in each of the watersheds. The flow rate causing the applied moment to be equal to the resisting moment is the upper limit of equation 23, which is discussed in the next subsection.

2.3. Minimum Cost Network Flow Optimization Problem

A comprehensive methodology to build and process data for this MILP decision support system is summarized in figure 6. Performing the hydrostatic and geotechnical calculations assesses whether a utility pole will fail at a given peak flow rate. An approximate water surface elevation (WSE) had to be determined at a cross section at the utility pole location. HEC-RAS 5.0.7 (HEC-RAS) was used to determine the WSEs at utility poles in each watershed.

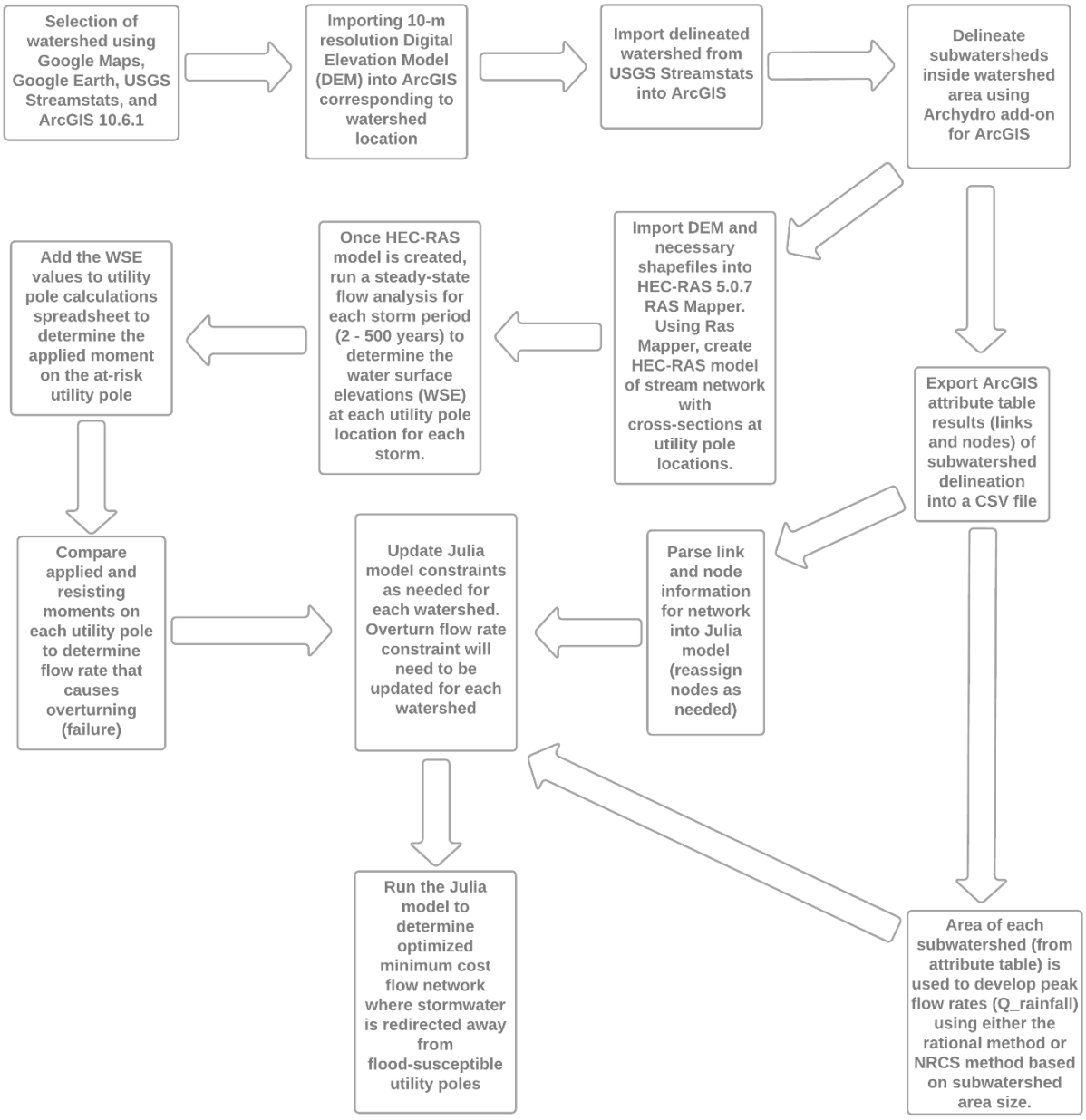

Fig 6. Methodology workflow to generate decision support system to mitigate flood water impact on utility poles

Flow across any network is governed by costs associated with production, some material in transit across the links, and a series of constraints applying to the links and nodes. Also, any optimization problem will consist of an objective function, decision variables, and constraints. This is the core anatomy of a network optimization problem. It is important to note that network

optimization problems can be applied to many other facets of life outside of electricity grid design and water resources infrastructure, e.g. (Durbin & Hoffman 2008), (Su et al. 2013).

Although many solvers exist for optimization problems, (Dunning et al. 2017) suggests that both the Gurobi solver and the JuMP interface are well-suited to MILP problems. To prevent utility pole failure, a minimum cost network flow problem will be established, where each watershed will be treated as a network of links and nodes. Each surface link (segment of stream) occupies one sub watershed and nodes are the vertices on either end of a stream segment. In the underground network, nodes are on either end of horizontal pipes.

$$\text{Min} \quad \Sigma_i Cost_i * U_i + \Sigma_p Cost_p * U_p \tag{17}$$

$Cost_i$ and $Cost_p$ are the cost of the vertical and horizontal pipe, respectively. Links in the subterranean network consist of:

1.) pipe extending vertically downward from surface nodes to connect to horizontal pipe and

2.) horizontal pipe conveying stormwater to the network outfall, or discharge point.

The vertical and horizontal pipe comprise the underground network. The optimal underground network is the target output of this model.

U_i is a binary decision variable that functions as either 0 or 1, depending on the existence of drainage at a node. U_p is a second binary decision variable, that dictates if there will be flow through an underground pipe or not. Flow rate units were calculated in cubic feet per second (cfs).

Equation 17 is the objective function for the minimum cost network flow problem and is subject to a series of constraints that define the feasible decision space. Equation 18 is for surface links that do not contain utility poles.

$$0 <= Q_{Stream} \tag{18}$$

$$0 <= Q_{drained} <= Q_{hydraulic\ capacity}\ (cfs) * U_i \quad (19)$$

$$0 <= Q_{pipe} <= Q_{hydraulic\ capacity}\ (cfs) * U_p \quad (20)$$

$Q_{hydraulic\ capacity}$ is expressed as the upper limit of equations 19 and 20 and can be used to size the vertical pipes connected to nodes and the horizontal underground pipes that will be used in the model. There are two conservation of flow constraints, one for surface network nodes and another for nodes in the underground network. Both of the conservation of flow constraints (equations 21 & 22) incorporate the Q_{stream}, $Q_{drained}$, and Q_{pipe} decision variables seen above. Q_{stream} refers to only the surface stream network. $Q_{drained}$ is used in equations 21 and 22 and is denoted in the surface network (equation 21) as $Q_{drained(i)}$ to determine the amount of stormwater to be conveyed into the vertical pipe at certain surface nodes so that utility pole failure is mitigated. In equation 22, $Q_{drained(p)}$ signifies stormwater in the underground network being conveyed downward through vertical pipe to the horizontal pipe. Once $Q_{drained(p)}$ reaches the horizontal pipe, it becomes Q_{pipe}, and is carried to the underground network's node of discharge (outfall).

It should be noted that $Q_{rainfall}$ becomes Q_{stream} in every subwatershed and flows into every downstream subwatershed.

Equation 21 is used to balance the network nodes on the surface and equation 22 balances the subterranean nodes. These two equations function in tandem with one another to connect the surface stream network to the vertical and horizontal pipes comprising the underground network. Essentially, the left side of equations 21 and 22 are stating that the flow of stormwater exiting a node at a link is subtracted by the flow of stormwater entering a node in the subsequent link and is equal to the net amount of stormwater at a particular node. Therefore, equations 21 and 22 are referred to as node balance equations, or flow conservation constraints.

$$\Sigma_j Q_{Stream(j,i)} - \Sigma_j Q_{Stream(i,j)} + Q_{rainfall} = Q_{drained(i)} + Discharge_{(i)} \quad (21)$$

$$\Sigma_j Q_{pipe(p,j)} - \Sigma_j Q_{pipe(j,p)} = Q_{drained(p)} - Discharge_{(p)} \quad (22)$$

Discharge represents stormwater leaving the network at a specified node both at the surface ($Discharge_{(i)}$) and in the underground pipe network ($Discharge_{(p)}$). For all networks in this study, discharge only occurs at the downstream terminal node.

Lastly, there are additional constraints for each of the utility pole locations, dictating that flow in a stream segment corresponding to a utility pole location cannot exceed the flow rate that would cause utility pole failure (overturning). Each of these constraints will take the following form and are crucial to the entire decision support system because they allow the model to decide how much stormwater to allocate to the underground network.

$$0 <= Q_{Stream}(location\ link) <= Failure\ Flow\ Rate\ (cfs) \quad (23)$$

Once water surface elevations were determined for each storm return period via a steady-state flow analysis in HEC-RAS, they were used to compute the moment being applied on the utility pole of interest. From there, the flow rate at which the utility pole failed is inferred. This flow rate is the upper limit of equation 23.

3. RESULTS

The methods enumerated above were applied to each watershed to test the model's efficacy on networks of different size and composition. The results of calculations for one utility pole in the Whittier, NC watershed (Table 3) are used as an example to illustrate a typical analysis for every utility pole. In Tables 4-6, the hydraulic capacity is the output of the model. "Drainage Capacity Recommended" is the amount of drainage occurring at a node for the model to reach the optimal solution. "Underground Pipe Flow" is the sum of surface drainage at a node and drainage occurring at any upstream nodes conveyed to that node.

Figures 7-9 were designed to be used as visual aids to interpret the data outputs in Tables 4-6, where locations of utility poles (red arrows) and underground pipe are clearly denoted. The nodes and links in figures 7-9 can also be referenced to exact locations within each watershed by using figures 2-4.

Table 3. Calculations template of parameters used to determine overturn flow rates *as the model constraints* for a flood-susceptible utility pole in Whittier, NC watershed

Utility Pole*	Storm Return Period (year)	[1]Flow Rate Colliding with Pole (ft^3/s)	[2]WSE (ft)	[3]Applied Moment (ft-lb)	[3]Resisting Moment (ft-lb)	Pass/Fail?	[1]Overturn Flow Rate (ft^3/s)
1	2	233.97	0.13	2109.61	26686.93	Pass	2959.91
1	5	297.41	0.18	4719.74	26686.93	Pass	1681.73
1	10	328.01	0.2	6378.83	26686.93	Pass	1372.35
1	25	387.83	0.39	17389.02	26686.93	Pass	595.22
1	50	425.5	0.46	24688.61	26686.93	Pass	459.96
1	100	468.72	0.54	35167.58	26686.93	Fail	355.70
1	500	569.1	0.61	58565.07	26686.93	Fail	259.34

*One utility pole was selected out of the 4 in the Whittier, NC watershed for demonstration purposes. **This analysis is typical for all at-risk utility poles at each of the watersheds.**

[1]1 ft^3/s = 0.028 m^3/s

[2]1 ft = 0.305 m

[3]1 ft-lb = 1.36 N-m

Some of the WSEs in Table 3 are high because the Whittier, NC watershed has a steep average slope and there are well-defined channels towards the confluence of the watershed's streams. These are where the flood-susceptible utility poles are located (Fig 7) and where cross-sections were taken in HEC-RAS.

In Tables 4-6, many of the node drainage values repeat, which is because the model is maximizing the amount of drainage occurring at nodes, so the optimized network has the fewest possible pipes with minimum deployment cost.

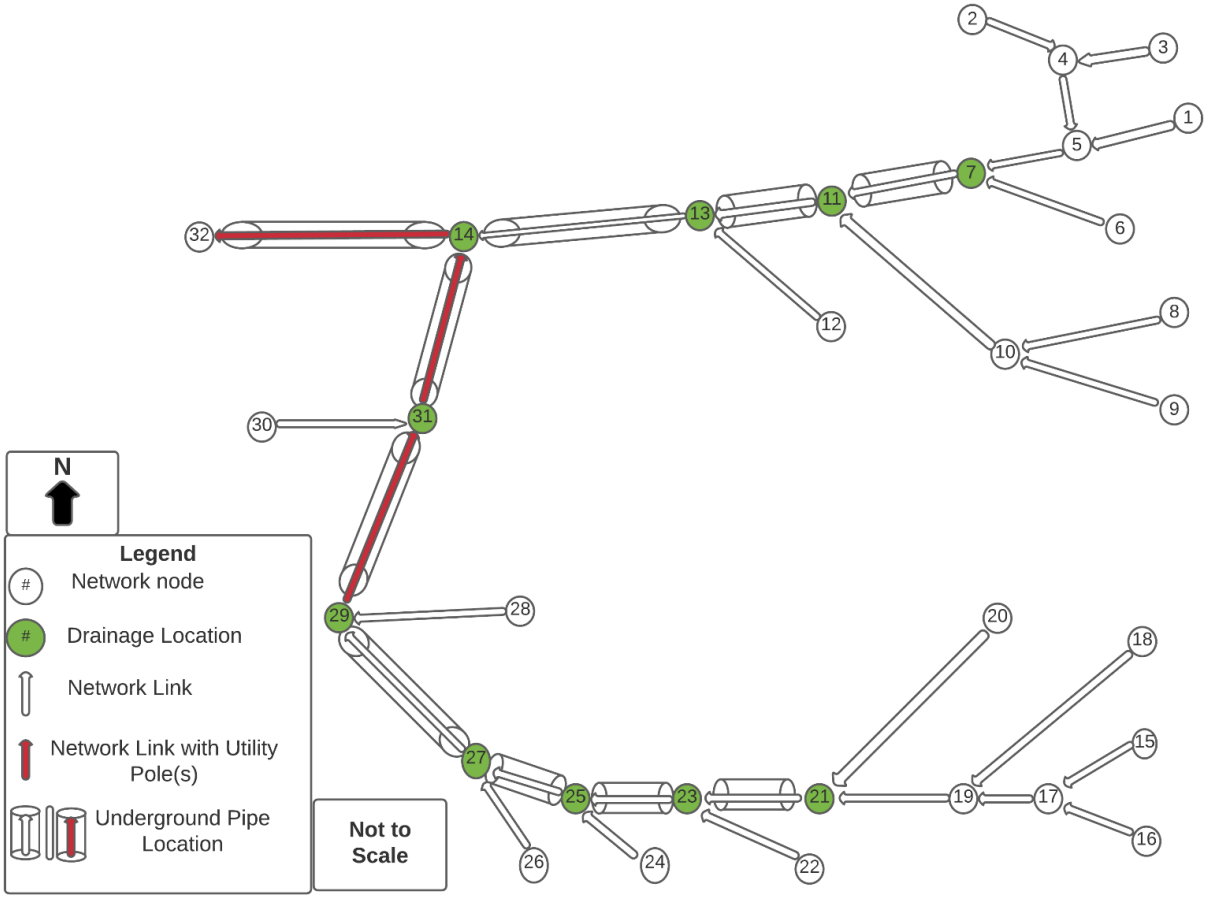

Fig 7. Whittier, NC Watershed Network Schematic for the 100-year Storm

Table 4. Optimized values for Whittier, NC watershed (Analysis for 100-year storm)

Node	[1]Drainage Capacity Recommended (ft^3/s)	Links	[2]Underground Pipe Flow (ft^3/s)
1		1,5	
2		2,4	
3		3,4	
4		4,5	
5		5,7	
6		6,7	
7	75.00	7,11	75.00
8		8,10	
9		9,10	
10		10,11	
11	75.00	11,13	150.00
12		12,13	
13	75.00	13,14	225.00
14	75.00	15,17	
15		16,17	
16		17,19	
17		18,19	
18		19,21	
19		20,21	
20		21,23	75.00
21	75.00	22,23	
22		23,25	127.04
23	52.04	24,25	
24		25,27	202.04
25	75.00	26,27	
26		27,29	277.04
27	75.00	28,29	
28		29,31	352.04
29	75.00	30,31	
30		31,14	427.04
31	75.00	14,32	727.04
32			

[1]Drainage Capacity Recommended is the amount of flow the model recommends be drained at a particular node to reach the optimal solution of the network optimization problem.

[2]Underground Pipe Flow is the sum of surface drainage from a node and existing pipe flow from surface drainage of upstream nodes. (notes 1 & 2 are typical for Tables 4-6).

Note: All blank areas indicate a flow of zero (typical for Tables 4-6).

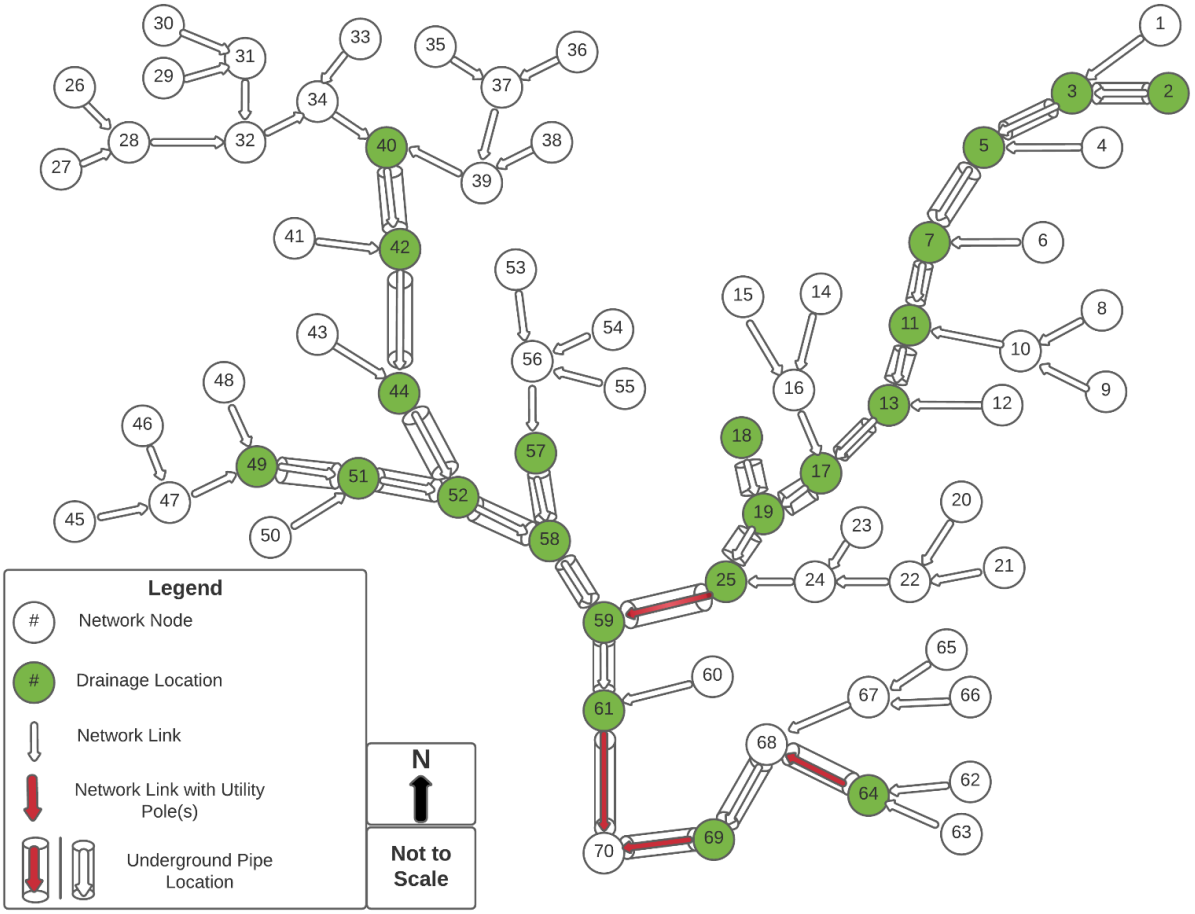

Fig 8. Leadville, CO Watershed Network Schematic for the 100-year Storm

529 **Table 5.** Optimization values for Leadville, CO watershed (Analysis for 100-yr storm)

Nodes	[1]Drainage Capacity Recommended (ft^3/s)	Links	[2]Underground pipe flow (ft^3/s)
1		1,3	
2	2375	2,3	2375
3	2375	3,5	4750
4		4,5	
5	2375	5,7	7125
6		6,7	
7	2375	7,11	9500
8		8,10	
9		9,10	
10		10,11	
11	2375	11,13	11875
12		12,13	
13	2375	13,17	14250
14		14,16	
15		15,16	
16		16,17	
17	2375	17,19	16625
18	112.10	18,19	112.10
19	2375	19,25	19112.10
20		20,22	
21		21,22	
22		22,24	
23		23,24	
24		24,25	
25	2375	26,28	
26		27,28	
27		28,32	
28		30,31	
29		29,31	
30		31,32	
31		32,34	
32		33,34	
33		35,37	
34		36,37	
35		37,39	
36		38,39	
37		39,40	
38		34,40	
39		40,42	2375
40	2375	41,42	
41		42,44	4750
42	2375	43,44	
43		44,52	7125

44	2375	45,47	
45		46,47	
46		47,49	
47		48,49	
48		49,51	178.75
49	178.75	50,51	
50		51,52	2553.75
51	2375	53,57	
52	2375	54,56	
53		55,56	
54		56,57	
55		57,58	952.81
56		52,58	12053.75
57	952.81	58,59	15381.57
58	2375	25,59	21487.10
59	2336.96	59,61	39205.63
60		60,61	
61	2375	62,64	
62		63,64	
63		64,68	484.43
64	484.43	65,67	
65		66,67	
66		67,68	
67		68,69	484.43
68		69,70	2195.88
69	1711.44	61,70	41580.63
70		[redacted]	

530

531

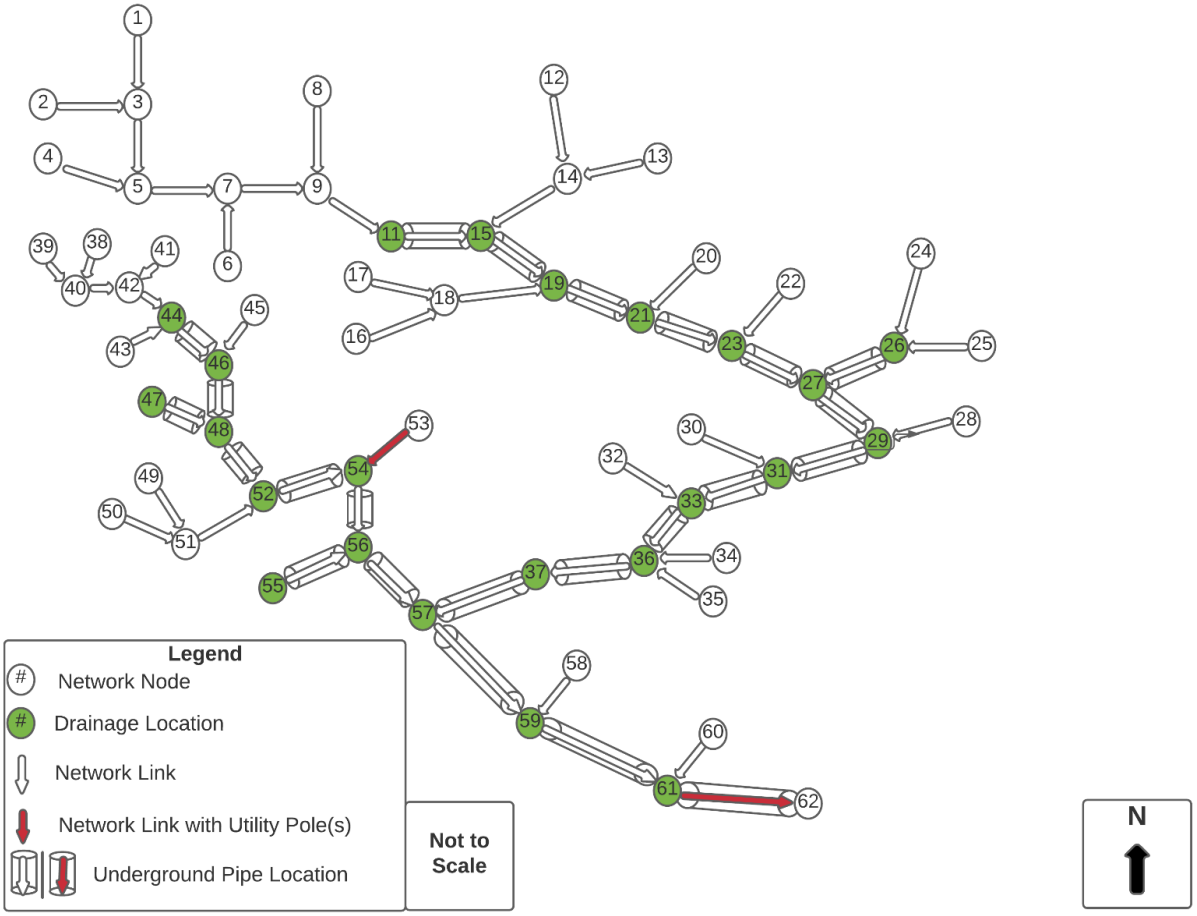

Fig 9. London, AR Watershed Network Schematic for 100-year Storm

546

547 **Table 6.** Optimization values for London, Arkansas watershed (Analysis run for 100-year storm)

Nodes	[1]Drainage Capacity Recommended (ft^3/s)	Links	[2]Underground Pipe Flow (ft^3/s)
1		1,3	
2		2,3	
3		3,5	
4		4,5	
5		5,7	
6		6,7	
7		7,9	
8		8,9	
9		9,11	
10		10,11	
11	1490	11,15	1490
12		12,14	
13		13,14	
14		14,15	
15	1490	15,19	2980
16		16,18	
17		17,18	
18		18,19	
19	1490	19,21	4470
20		20,21	
21	1490	21,23	5960
22		22,23	
23	1490	23,27	7450
24		24,26	
25		25,26	
26	1490	26,27	1490
27	1490	27,29	10430
28		28,29	
29	1490	29,31	11920
30		30,31	
31	1490	31,33	13410
32		32,33	
33	1490	33,36	14900
34		34,36	
35		35,36	
36	1349.02	36,37	16249.02
37	1490	38,40	
38		39,40	
39		40,42	
40		41,42	
41		42,44	
42		43,44	

43		44,46	1490
44	1490	45,46	
45		46,48	2891.27
46	1401.27	47,48	843.03
47	843.03	48,52	5222.30
48	1490	49,51	
49		50,51	
50		51,52	
51		52,54	6714.30
52	1490	53,54	
53		54,56	8202.30
54	1490	55,56	1490
55	1490	56,57	11184.30
56	1490	37,57	17739.02
57	1490	57,59	30413.33
58		58,59	
59	1490	59,61	31903.33
60		60,61	
61	1490	61,62	33393.33
62			

548

549 ## 4. DISCUSSIONS AND CONCLUSIONS

550

551 The model is behaving as expected for each of the watersheds. Sufficient drainage is
552 occurring at nodes (Drainage Capacity Recommended) to mitigate utility pole failure. In the
553 Whittier, NC watershed, this will allow successively larger underground pipes to convey flood
554 water away from utility poles. The hydraulic capacities reported in Table 4 were a result of flow
555 rates from the 100-year storm and are appropriate for feasible pipe diameters. In the Leadville, CO
556 and London, AR watersheds, peak flow rates for the 100-year storm were much higher due to
557 larger subwatershed areas. Therefore, the model is reporting large hydraulic capacities for node
558 drainage and underground pipe flow (Tables 5 and 6) that are not conducive to feasible pipe
559 diameters. This means that utility poles in the Leadville, CO and London, AR watersheds are at
560 great risk of failure during severe flooding events and to mitigate this failure using the current

framework would require unreasonably large vertical and horizontal pipes. To resolve this issue, one can adopt alternative measures, including changes in the utility distribution line types (e.g. installing lines underground), which is beyond the scope of our particular study.

Based on the outputs of the model in Tables 5 and 6, it is recommended that any future versions of this study delineate smaller subwatersheds inside the two larger watersheds. Smaller subwatersheds would result in lower peak flow rates and a larger network. Therefore, a more robust decision support system would also be created where the hydraulic capacity results would be conducive to feasible pipe diameters.

The present decision support system could be further strengthened by adding more decision variables. An additional decision variable could be added at certain nodes for above-ground hydraulic structures, such as trapezoidal channels. These channels can convey high peak flow rates and would be feasible in the Leadville, CO and London, AR watersheds due to existing lakes. The channels' conveyance of high peak flow rates would lessen the load on the optimal underground pipe network. In Tables 4-6, many of the node drainage values repeat. This is because the model is maximizing the amount of drainage occurring at nodes, so the optimized network has the fewest possible pipes with minimum deployment cost.

Nearly all the utility poles analyzed for the 100-year storm were projected to fail based on the calculations (refer to Table 3 for calculation result template). However, the utility pole at link 53,54 in the London, AR watershed passed. As seen in figure 9, the model deemed drainage to be unnecessary at node 53 because the constraint summarized in equation 23 was not violated. This was due to a low peak flow rate in the link's corresponding subwatershed.

Future studies should consider a more thorough methodology for flood-susceptible utility pole identification. (Alam et al. 2020) devised a methodology to determine utility pole vitality

584 through photography from unmanned aerial vehicles (UAVs) and computation of "computer
585 vision-based" angles of inclination. Post-computation, utility poles with angles of inclination
586 reflecting an unhealthy condition (>10°) can be identified. After identification, the framework
587 introduced in this study could be applied so that any failure due to flooding is mitigated.

588 Photography from UAVs could also strengthen the techniques proposed in this study. There
589 are commercially available software packages (Ansys Workbench and O-Calc Pro Line Design)
590 that use photogrammetry to determine accurate measurement of objects. Utility pole photography
591 could be analyzed in either of these programs to determine more accurate measurements of
592 diameter, circumference, and length of pole, which factor into calculations for the total resisting
593 moment. A more accurately calculated resisting moment will produce an even more reliable
594 analysis of utility pole failure.

595 The results of this MILP optimization framework, using the Gurobi solver inside the JuMP
596 interface, are encouraging because the model has demonstrated the ability to successfully redirect
597 flood waters from at-risk utility poles. Therefore, the novel methodology proposed in this study
598 can alleviate flood vulnerabilities in the U.S. electricity grid and abroad.

599

600 # 5. DECLARATIONS

601 **Ethical Approval**: Obviously, this article is not about life science and does not contain any
602 studies involving human participants performed by any of the authors.

603 **Consent to Participate:** Obviously, this article is not about life science and does not contain any
604 studies involving human participants performed by any of the authors.

605 **Consent to Publish:** Obviously, this article is not about life science and does not contain any
606 studies involving human participants performed by any of the authors.

Authors Contributions: HT-D. Formulating the research questions and data collection. MV. Implementing the optimization model and writing the draft manuscript. SM. Supervising the analyses and reviewing the manuscript and visualizations.

Funding: The work submitted for publication is un-funded.

Conflicts of Interest/Competing Interests: The submitted article represents an original scientific work that has not been published and is not under consideration for publication elsewhere. All works referred to in the article have been acknowledged by proper citation, and there is no real or apparent conflict of interests in its content. There is no financial or non-financial interests that are directly or indirectly related to the work submitted for publication. The work submitted for publication is un-funded.

Availability of data and materials: All data, models, or code that support the findings of this study are available from the corresponding author upon reasonable request.

6. REFERENCES

Al-Shammary, A. A. G., Kouzani, A. Z., Kaynak, A., Khoo, S. Y., Norton, M., and Gates, W. (2018). "Soil Bulk Density Estimation Methods: A Review." Pedosphere, 28(4), 581-596.

Alam, M. M., Zhu, Z., Eren Tokgoz, B., Zhang, J., and Hwang, S. (2020). "Automatic Assessment and Prediction of the Resilience of Utility Poles Using Unmanned Aerial Vehicles and Computer Vision Techniques." International Journal of Disaster Risk Science, 11(1), 119-132.

Alqattan, N. A. (2014). "A Multi-Period Mixed Integer Linear Programming Model for Desalination and Electricity Co-generation in Kuwait."

Anderson, G. B., and Bell, M. L. (2012). "Lights Out: Impact of the August 2003 Power Outage on Mortality in New York, NY." Epidemiology, 23(2), 189-193.

Andrews, E. S., Chung, F. I., and Lund, J. R. (1992). "Multilayered, Priority‐Based Simulation Of Conjunctive Facilities." Journal of Water Resources Planning and Management, 118(1), 32-53.

Bareither, C. A., Edil, T. B., Benson, C. H., and Mickelson, D. M. (2008). "Geological and Physical Factors Affecting the Friction Angle of Compacted Sands." Journal of Geotechnical and Geoenvironmental Engineering, 134(10), 1476-1489.
Bieupoude, P., Azoumah, Y., and Neveu, P. (2012). "Optimization of drinking water distribution networks: Computer-based methods and constructal design." Computers, Environment and Urban Systems, 36(5), 434-444.
Bixby, R. (2012). "A Brief History of Linear and Mixed-Integer Programming Computation."
Campbell, R. J., and Lowry, S. "Weather-related power outages and electric system resiliency."
Carini, M., Maiolo, M., Pantusa, D., Chiaravalloti, F., and Capano, G. (2018). "Modelling and optimization of least-cost water distribution networks with multiple supply sources and users." Ricerche di Matematica, 67(2), 465-479.
Charlotte-Mecklenburg Stormwater Services. 2014 Charlotte-Mecklenburg Storm Water Design Manual Chapter 2. Charlotte Chamber Design Manual Task Force. https://charlottenc.gov/StormWater/Regulations/Documents/SWDMC/SWDMChap2Final12312013.pdf (accessed 27 January 2021)
City of Colorado Springs. 2014 Drainage Criteria Manual Vol I. https://coloradosprings.gov/sites/default/files/images/dcm_volume_1.pdf (accessed 27 January 2021)
City of Fayetteville Engineering Division. 2014 Fayetteville Arkansas Drainage Criteria Manual. https://www.fayetteville-ar.gov/DocumentCenter/View/2248/Drainage-Criteria-Manual-2014-PDF (accessed 27 January 2021)
Crucitti, P., Latora, V., and Marchiori, M. (2004). "Model for cascading failures in complex networks." Physical Review E, 69(4), 045104.
Das, B. M. (2016). Principles of foundation engineering (8th ed., pp. 593–645). Boston, Ma Cengage Learning.
Davisson, M., and Prakash, S. (1963). "A review of soil-pole behavior." Highway Research Record(39).
Dunning, I., Huchette, J., and Lubin, M. (2017). "JuMP: A Modeling Language for Mathematical Optimization." SIAM Review, 59(2), 295-320.
Durbin, M., and Hoffman, K. (2008). "OR PRACTICE—The Dance of the Thirty-Ton Trucks: Dispatching and Scheduling in a Dynamic Environment." Operations Research, 56, 3-19.
Evenson, D. E., and Moseley, J. C. (1970). "SIMULATION/OPTIMIZATION TECHNIQUES FOR MULTI-BASIN WATER RESOURCE PLANNING1." JAWRA Journal of the American Water Resources Association, 6(5), 725-736.
Ghelichi, Z., Tajik, J., and Pishvaee, M. S. (2018). "A novel robust optimization approach for an integrated municipal water distribution system design under uncertainty: A case study of Mashhad." Computers & Chemical Engineering, 110, 13-34.
Groisman, P. Y., Knight, R. W., and Karl, T. R. (2012). "Changes in intense precipitation over the central United States." Journal of Hydrometeorology, 13(1), 47-66.
Hemme, K. (2015). "Critical infrastructure protection: Maintenance is national security." Journal of Strategic Security, 8(3), 25-39.
Hines, P., Apt, J., and Talukdar, S. (2008) "Trends in the history of large blackouts in the United States." 2008 IEEE Power and Energy Society General Meeting-Conversion and Delivery of Electrical Energy in the 21st Century, 1-8.
Ilich, N. (2009). "Limitations of Network Flow Algorithms in River Basin Modeling." Journal of Water Resources Planning and Management, 135(1), 48-55.

680 Keshavarzian, M. (2002). "Self-supported Wood Pole Fixity at ANSI Groundline." Practice
681 Periodical on Structural Design and Construction, 7(4), 147-155.
682 Klinger, C., and Owen Landeg, V. M. (2014). "Power outages, extreme events and health: a
683 systematic review of the literature from 2011-2012." PLoS currents, 6.
684 Koloski, J. W., Schwarz, S. D., & Tubbs, D. W. (1989). Geotechnical Properties of Geologic
685 Materials. http://www.tubbs.com/geotech/geotech.htm (accessed 20 January 2021)
686 Labadie, J. W., Bode, D. A., and Pineda, A. M. (1986). "NETWORK MODEL FOR
687 DECISIONSUPPORT IN MUNICIPAL RAW WATER SUPPLY1." JAWRA Journal of
688 the American Water Resources Association, 22(6), 927-940.
689 Li, Z., and Guo, J. (2006). "Wisdom about age [aging electricity infrastructure]." IEEE Power
690 and Energy Magazine, 4(3), 44-51.
691 Liu, S., Konstantopoulou, F., Gikas, P., and Papageorgiou, L. G. (2011). "A mixed integer
692 optimisation approach for integrated water resources management." Computers &
693 Chemical Engineering, 35(5), 858-875.
694 Lubchenco, J., and Hayes, J. (2012). "A better eye on the storm." Scientific American, 306(5),
695 68-73.
696 Mani, A., Tsai, F. T.-C., and Paudel, K. P. (2016). "Mixed Integer Linear Fractional
697 Programming for Conjunctive Use of Surface Water and Groundwater." Journal of Water
698 Resources Planning and Management, 142(11), 04016045.
699 Manshadi, S., and Khodayar, M. (2015). "Resilient Operation of Multiple Energy Carrier
700 Microgrids." IEEE Transactions on Smart Grid, 6.
701 Manshadi, S., and Khodayar, M. (2018). "Preventive reinforcement under uncertainty for
702 islanded microgrids with electricity and natural gas networks." Journal of Modern Power
703 Systems and Clean Energy, 6, 1-11.
704 Maringanti, C., Chaubey, I., Arabi, M., and Engel, B. (2011). "Application of a Multi-Objective
705 Optimization Method to Provide Least Cost Alternatives for NPS Pollution Control."
706 Environmental Management, 48(3), 448-461.
707 Marx, M. A., Rodriguez, C. V., Greenko, J., Das, D., Heffernan, R., Karpati, A. M., Mostashari,
708 F., Balter, S., Layton, M., and Weiss, D. (2006). "Diarrheal illness detected through
709 syndromic surveillance after a massive power outage: New York City, August 2003."
710 American Journal of Public Health, 96(3), 547-553.
711 McLaughlin, K. (2020, May 20). Photos and videos show the destruction after 2 dams collapsed
712 in Michigan, threatening a town with 9 feet of flooding. Insider.
713 https://www.insider.com/photos-videos-show-michigan-dam-collapse-destruction-2020-5
714 Merwade, V. (2010). "Creating SCS Curve Number Grid using HEC-GeoHMS."
715 Muleta, M. K., and Nicklow, J. W. (2002). "Evolutionary algorithms for multiobjective
716 evaluation of watershed management decisions." Journal of Hydroinformatics, 4(2), 83-
717 97.
718 Pant, R., Thacker, S., Hall, J. W., Alderson, D., and Barr, S. (2018). "Critical infrastructure
719 impact assessment due to flood exposure." Journal of Flood Risk Management, 11(1), 22-
720 33.
721 Sigvaldson, O. T. (1976). "A simulation model for operating a multipurpose multireservoir
722 system." Water Resources Research, 12(2), 263-278.
723 Su, L.-H., Cheng, T. C. E., and Chou, F.-D. (2013). "A minimum-cost network flow approach to
724 preemptive parallel-machine scheduling." Computers & Industrial Engineering, 64(1),
725 453-458.

Teegavarapu, R. S. (2017). "Climate variability and changes in precipitation extremes and characteristics." Sustainable Water Resources Planning and Management Under Climate Change, Springer, 3-37.

Trenberth, K. E. (2011). "Changes in precipitation with climate change." Climate Research, 47(1-2), 123-138.

Turnquist, M., and Vugrin, E. (2013). "Design for resilience in infrastructure distribution networks." Environment Systems & Decisions, 33(1), 104-120.

USDA Forest Service Engineering Staff. (1994). Slope Stability Reference Guide for National Forests in the United States. USDA. https://www.fs.fed.us/rm/pubs_other/wo_em7170_13/wo_em7170_13_vol2.pdf (accessed 20 January 2021)

USDA NRCS. (n.d.). Soil Bulk Density/Moisture/Aeration. USDA-NRCS. https://www.nrcs.usda.gov/Internet/FSE_DOCUMENTS/nrcs142p2_053260.pdf (accessed 20 January 2021)

U.S. Geological Survey, City of Charlotte and Mecklenburg County, & Weaver, J. (2006). Frequency of Annual Maximum Precipitation in the City of Charlotte and Mecklenburg County, North Carolina, through 2004. In . https://pubs.usgs.gov/sir/2006/5017/pdf/report.pdf (accessed 20 January 2021)

Veintimilla-Reyes, J., Cattrysse, D., De Meyer, A., and Van Orshoven, J. (2016). "Mixed integer linear programming (MILP) approach to deal with spatio-temporal water allocation." Procedia Eng, 162, 221-229.

Watson, J.-P., Greenberg, H. J., and Hart, W. E. (2004). "A Multiple-Objective Analysis of Sensor Placement Optimization in Water Networks." Critical Transitions in Water and Environmental Resources Management, 1-10.

Wolfe, R. W., and Moody, R. C. "ANSI Pole Standards: Development and Maintenance." Proceedings of the first Southeastern pole Conference. For. Prod. Society. Madison, USA, 143-149.